SUPPORTING INFORMATION

Interactions between Redox Complexes and Semiconductor Quantum Dots Coupled via a Peptide Bridge

Igor L. Medintz, Thomas Pons, Scott A. Trammell, Amy F. Grimes, Doug S. English, Juan B. Blanco-Canosa, Philip E. Dawson, and Hedi Mattoussi

Table SI. Anodic potentials of selected QD samples together with those of metal-complex-labeled peptides. Single layers on PAH-modified ITO in PBS were used.

Compound	**Anodic peak potentials, V vs Ag/AgCl** [a]
590-nm DHLA-PEG	0.2
590-nm DHLA	0.21
540-nm DHLA-PEG	0.235
540-nm DHLA	0.217
Ru-phen-peptide	0.23
Fc-peptide	0.46
Ru-bpy-phen-peptide	1.16

[a] peak potentials measured at 50 mV/s.

Table SII. Formal potential of selected metal-complexes.

Compound	**Formal potential E_f, V**
$Ru(NH_3)_4(phen\text{-}mal)^{2+}$	0.609[a]
$Ru(NH_3)_4(phen\text{-}mal)^{2+}$	0.291[b]
$Ru(NH_3)_4(phen\text{-}mal)^{2+}$	0.263[c]
Ru-phen-peptide	0.223[d]
Ferrocene	0.307[e]
Ferrocene-COOH	0.325[f]
Ferrocene-peptide	0.440[g]
Ru-bpy-phen	1.32[e]

[a] E_f vs SCE (Saturated Calomel Electrode) in DMF at a glassy carbon electrode (Trammell, Goldston et al. 2001)
[b] E_f vs SCE in acetonitrile at a glassy carbon electrode (Trammell, Goldston et al. 2001)
[c,d,f,g] E_f vs Ag/AgCl calculated from average of the anodic and cathodic peak potentials from cyclic voltammograms measured in PBS buffer at a PAH modified ITO electrode and for Ru- or Fe-labeled peptide adsorbed at the electrode.
[e] E_f vs SCE in acetonitrile (Bard, A. J.; Faulkner, L. R., *Electrochemical Methods: Fundamentals and Applications*. Wiley: New York, 1980).

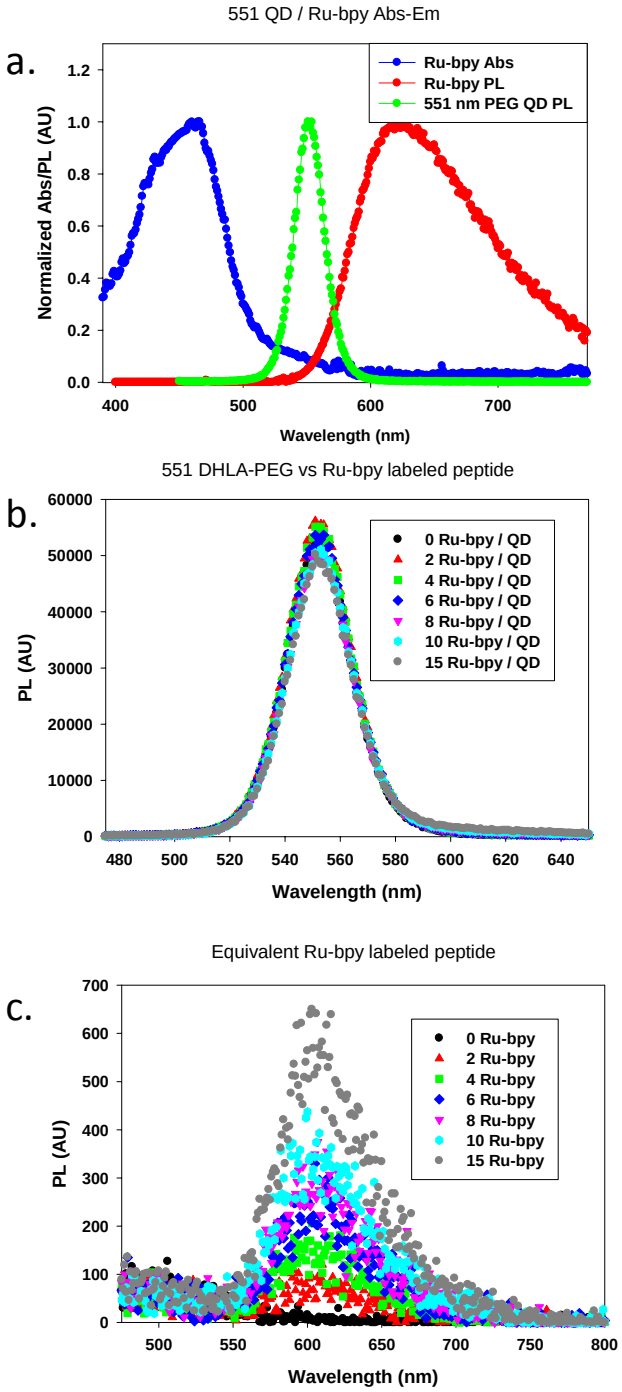

Figure S1. Characterization of Ru-bpy-phen and QD-peptide-Ru-bpy-phen assemblies. (a) Normalized absorption and PL of Ru-bpy-phen together with the normalized PL of 551-nm emitting QDs. (b) PL evolution of DHLA-PEG-QDs conjugated with increasing number of the Ru-bpy-phen-labeled glutathione modified peptides. (c) Direct excitation PL of equivalent amounts of Ru-bpy-phen-labeled peptide (control). This indicates that contribution of Ru-bpy-phen to the overall QD PL signal is extremely small. Samples were excited at 300 nm.

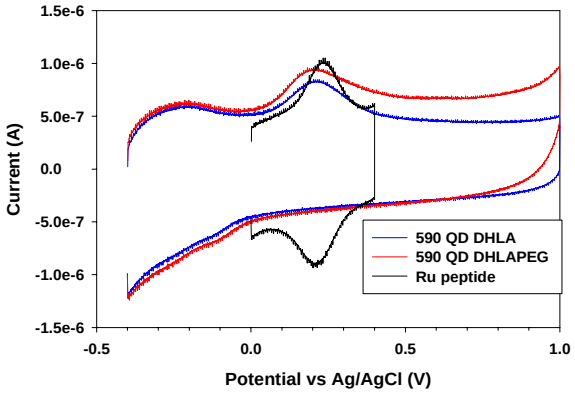

Figure S2. Representative raw (uncorrected) CV plots corresponding to the data shown in Figure 2.

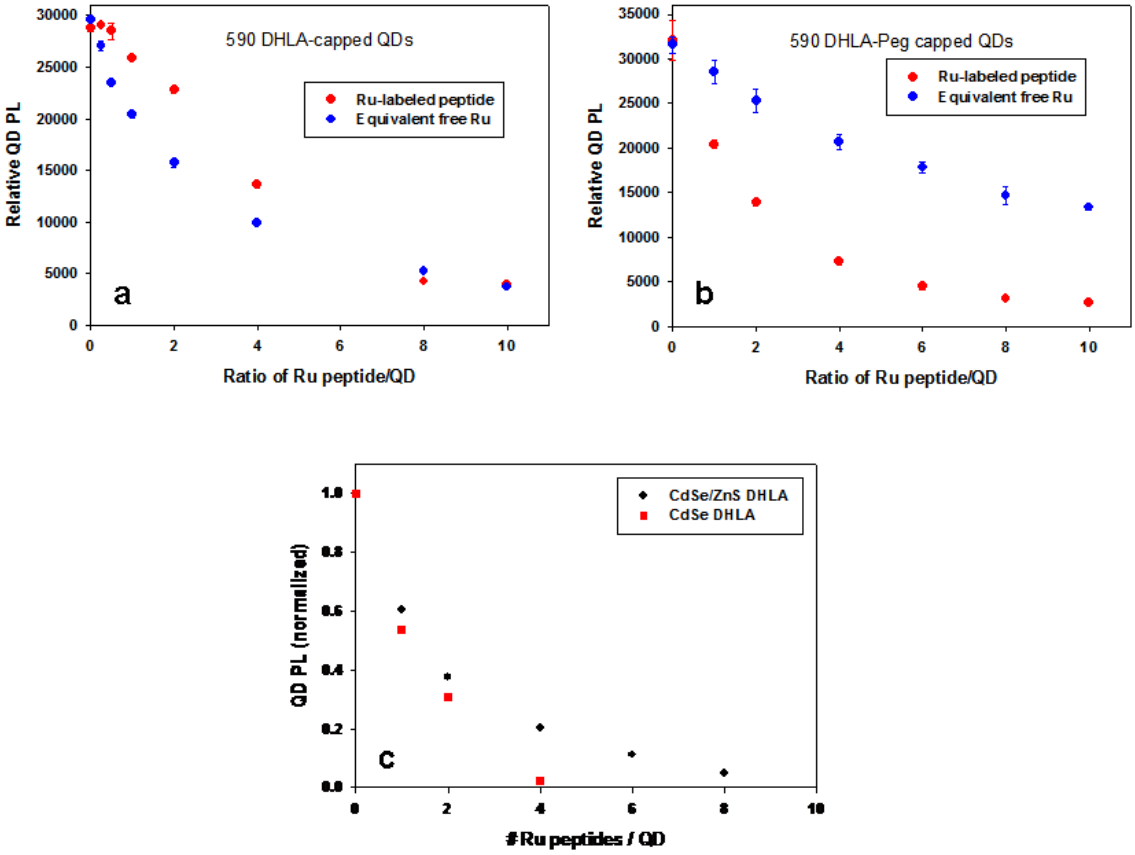

Figure S3. Control PL quenching experiments. (a) PL of 590 nm-emitting DHLA-QDs mixed with increasing molar ratios of either Ru-phen-labeled His-peptide or an equivalent amount of free Ru-phen. (b) The corresponding PL progression for samples using DHLA-PEG-QDs. (c) Side-by-side comparison of the quenching of CdSe-ZnS core-shell and CdSe core-only DHLA-QDs assembled with increasing number of Ru-phen-labeled peptides.

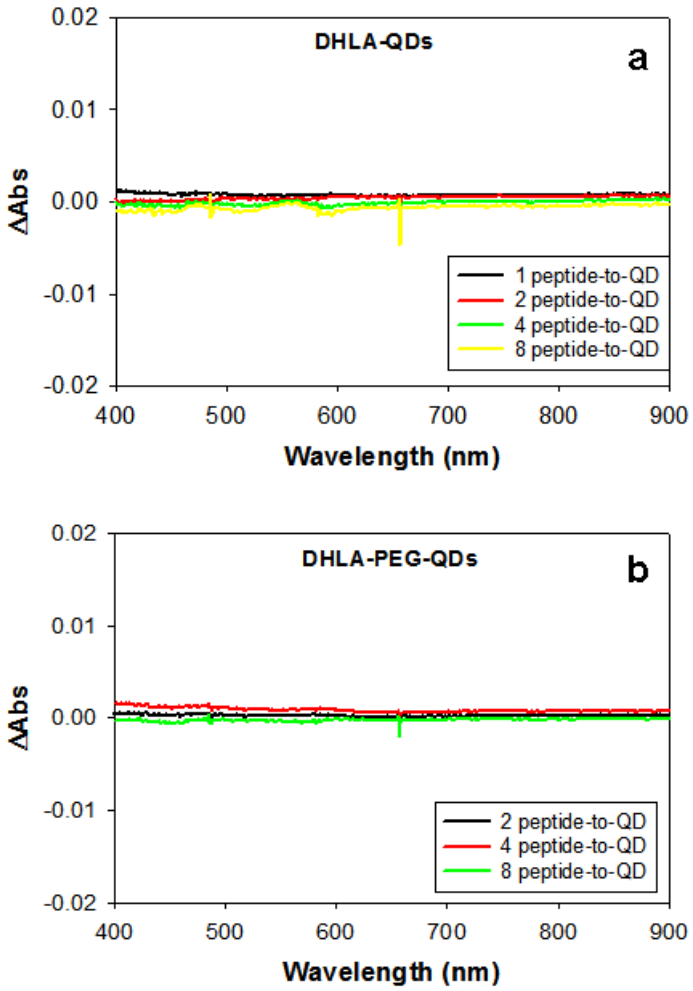

Figure S4. Differential absorption spectra ΔAbs of **(a)** DHLA-QDs and **(b)** DHLA-PEG-QDs self-assembled with the indicated number of unlabeled peptides per QD; 590 nm-emitting QDs were used. The data indicate that changes in the absorption are not induced by the peptides.

Proteolytic Assays. For the proteolytic assay, bovine plasma thrombin (EC 3.4.21.5, specific activity 24.5 NIH units/mg-solid), α-chymotrypsin from bovine pancreas (EC 3.4.21.1, specific activity of 61 units/mg protein) and chymostatin were obtained from Sigma. Appropriate aliquots of the QD-peptide stock solution were diluted into microtiter wells containing the desired concentrations of enzyme and PL spectra were collected before and after digestion using the plate reader. All assays were performed in triplicate, and standard deviations are shown where appropriate. Additional details on self-assembly, proteolytic assay format, protease specificity, data analysis, derivation of enzymatic activity and Michaelis-Menten parameters K_M and V_{max} were previously described in reference (Medintz, Clapp et al. 2006) using the following expressions (Bowden 1995):

$$V = \frac{d[P]}{dt} = \frac{V_{max}[E]}{K_M + [E]}$$

and

$$V = \frac{d[P]}{dt} = \frac{V_{\max}^{app}[E]}{K_M^{app} + [E]}$$ in the presence of an inhibitor

Where $[P]$, $[E]$ respectively designate the product (digested substrate) and enzyme concentrations.

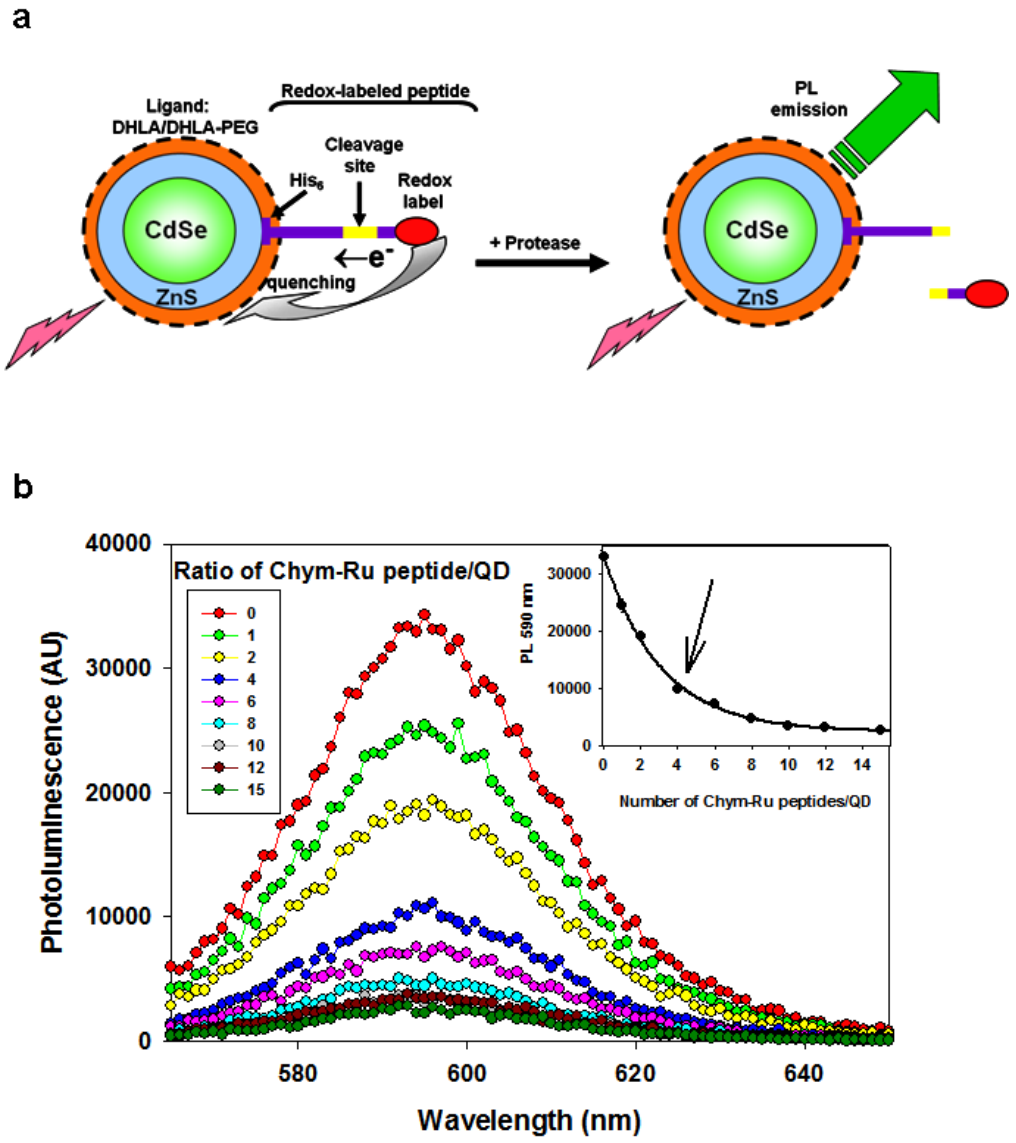

Figure S5. (a) Schematic representation of the proteolytic enzyme sensing mechanism based on charge transfer interactions. **(b)** Progression of the PL spectra of 590-nm emitting QDs conjugated with increasing number of Chym-Ru peptides. The inset shows the corresponding PL at the peak value vs. Chym-Ru-to-QD ratio (standard curve).

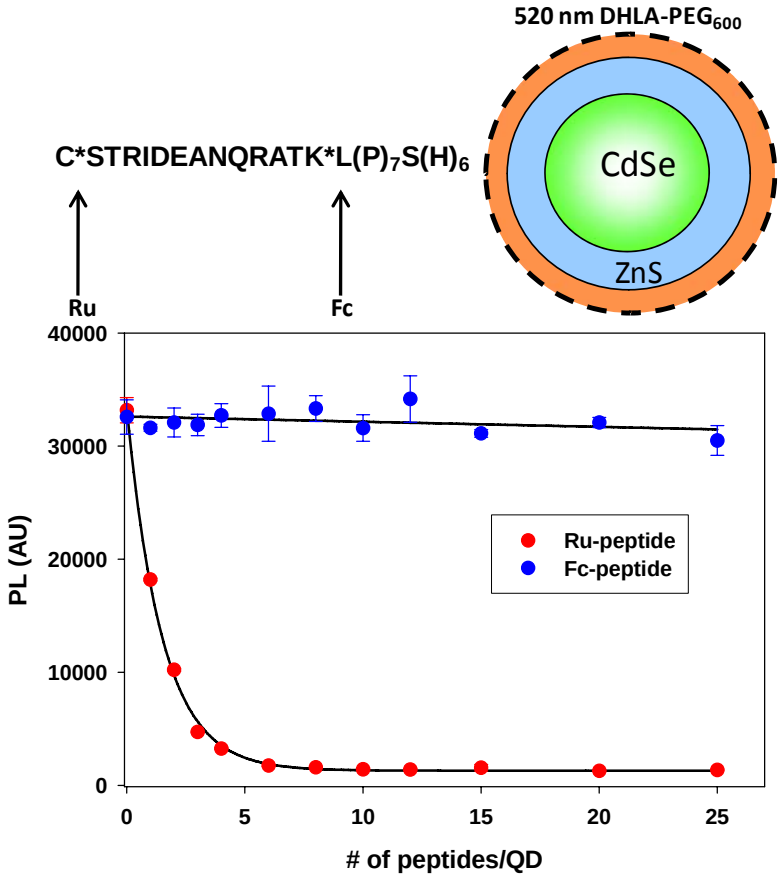

Figure S6. Testing the potential through-bond peptide contribution to charge transfer interactions. The shown peptide was labeled with either Ru-phen-complex at the distal cysteine (C) or with Fc-complex at the closer lysine (K) residue. PL of the QDs was monitored for increasing ratios of peptide-metal-complex per QD-conjugate. Data clearly indicate that the peptide sequence does not determine the charge transfer rate and the ensuing PL quenching efficiency.

Effects of adding $FeSO_4$ salt. PL quenching: 552-nm emitting DHLA-QDs were added to phosphate buffered saline (PBS) at pH 6.5 at a 250 nM, and supplemented with Fe(II)SO_4 salt (Sigma-Aldrich) at the indicated concentrations. The slightly acidic pH was used to prevent the transformation of Fe ions into $Fe(OH)_3$ which becomes problematic at ~ pH 7 (Laitinen and Harris, 1975). The relative QD PL was then measured on the Tecan Plate Reader from triplicate samples using 325-nm excitation and compared to control samples without $FeSO_4$. Similarly, the differential absorption spectra were measured for solutions of QDs at 830 nM, QDs mixed with $FeSO_4$, and $FeSO_4$ control-only using a UV-Vis HP 8453 diode array spectrophotometer (Agilent technologies, Santa Clara, CA).

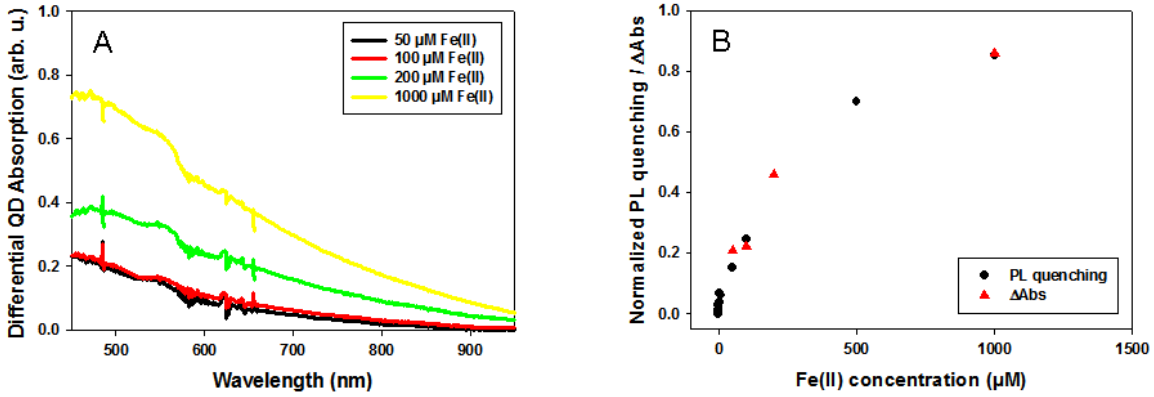

Figure S7. A. Differential QD absorption spectra upon addition of different Fe(II) concentration. B. Normalized PL quenching and amplitude of the QD differential absorption spectrum as a function of Fe(II) concentration.

Marcus electron transfer concept

Within the framework of Marcus theory, the rate of the electron transfer is given by equation 1 (Lippard et al.; Marcus et al.):

$$k_{et} = (4\pi^2/h)T_{DA}^2(FC) = (4\pi^2/h)\, T^o{}_{DA}^2 \exp(-\beta(R-R_o))\,(FC), \qquad (1)$$

where h is the Planck constant, T^0_{DA} is the tunneling matrix element accounting for the electronic coupling between the reductant (donor) and oxidant (acceptor) at the van der Waals contact distance. FC is the Frank-Condon factor which is a measure of the nuclear motion involved in the electron-transfer process. The transfer rate has an exponential dependence on the separation distance ($R-R_0$), with β depicting how the medium affects the electron tunneling between the donor and acceptor. R_0 is the van der Waals contact distance. For proteins β is in the range of 1.4 $Å^{-1}$.

The FC term is based on Marcus theory:

$$FC = (4\pi\lambda k_B T)^{-1/2} \exp[-(\Delta G^o+\lambda)^2/4\lambda k_B T]. \qquad (2)$$

The exponential term in equation 2 accounts for the strong dependence of transfer rate on changes in the free energy, ΔG^o, and the total reorganizational energy, λ. ΔG^o is directly related to the difference in redox potentials between donor and acceptor; λ corresponds to the energy needed to distort the starting reactants into the geometry of the products and the reorganization of the solvent. k_B is the Boltzmann constant.

In our case, the donors are the metal complexes and the acceptors are the QDs. If we assume the measured QD PL loss is related to charge (electron) transfer, then we can conclude that as the oxidation potential of the metal complexes becomes less positive (meaning lower ionization potential), the driving force of electron transfer to the QD surface states is increased, and that would increase the rate of charge transfer and

consequently rate of QD PL loss. Thus, complexes with lower oxidation potentials (e.g., Ru-phen) produce a ratio-dependent PL quenching, whereas those with higher oxidation potentials (e.g., ferrocene) do not produce CT and PL loss.

References

Bowden, A.C. Fundamentals of Enzyme Kinetics. London, Portland Press Limited (1995).

Medintz, I.L., Dawson, P.E., Clapp, A.R., Uyeda, H.T., Chang, E.L., Deschamps, J.R. & Mattoussi, H. Proteolytic activity monitored by fluorescence resonance energy transfer through quantum-dot-peptide conjugates. *Nat. Mater.* **2006**, 5, 581-589..

Trammell, S.A., Goldston, Jr., H.M., Tran, P.T., Tender, L.M., Conrad, D.W., Benson, D.E. and Hellinga, H.W. Synthesis and characterization of a ruthenium(II)-based redox conjugate for reagentless biosensing. *Bioconj. Chem.* **2001**, 12, 643-647.

Laitinen, H.A. and Harris, W.E. Chemical Analysis. An Advanced Test and Reference. 2nd Edition. McGraw-Hill, Inc. New York, 1975.

Lippard, S. J.; Berg, J. M., *Principles of Bioinorganic Chemistry*. University Science Books: Mill Valley, Calif., 1994.

Marcus, R.A.; Sutin N. "Electron transfers in chemistry and biology". *Biochim. Biophys. Acta.* **811,** 265 (1985).